MODELLING A LINEAR PM MOTOR INCLUDING MAGNETIC SATURATION

H. Polinder[1], J.G. Slootweg[1], J.C. Compter[2], M.J. Hoeijmakers[1]

[1] Delft University of Technology, The Netherlands, [2] Eindhoven University of Technology, The Netherlands

ABSTRACT

The use of linear permanent-magnet (PM) actuators increases in a wide variety of applications because of the high force density, robustness and accuracy. The paper describes the modelling of a linear PM motor applied in, for example, wafer steppers, including magnetic saturation. This is important because to reach high performance, the feed-forward control must predict the force generated by the motor, also when the motor is saturated. The motor is modelled as a reluctance network. The saturating parts of the magnetic circuit are modelled as variable reluctances and magnetomotive forces represent the currents and the magnets. In saturation, a current leading the no-load voltage results in an increase of the generated force. The good correlation between the calculated and the measured force justifies the model.

1 INTRODUCTION

A trend to increase the use of linear electro mechanic actuators can be observed in a wide range of applications, from aeroplanes (fly by wire) to factory automation, as described by Gieras and Piech [1]. Important advantages of linear electro mechanic actuators are that they are clean, robust, and efficient and that they can be fed from simple copper wires. Further, direct-drive actuators can have a high positioning and speed accuracy because the problems of a mechanic transmission are omitted.

A very demanding application of linear electro mechanic actuators is in wafer steppers. An extreme positioning accuracy (on the nanometre level) has to be combined with a high throughput in an ultra clean environment.

For these demanding applications, the linear motors are mostly of the permanent magnet type, because compared to other linear electric motors, they have a high force density, a high efficiency and a relatively simple control. This paper deals with a linear permanent-magnet (PM) motor applied for horizontal micrometre positioning in, for example, wafer steppers and component placing machines. Most of the time, such a motor is not heavily loaded, but during short intervals of large acceleration, it is heavily loaded. During these short intervals, the magnetic circuit of the motor may saturate. To control the system accurately and with a high performance, feed-forward control is used. This feed-forward control must predict the force developed by the motor.

Therefore, the objective of this paper is to derive a model to calculate the force under saturated conditions and to validate this model experimentally. This is done in such a way that the method can already be used in the design phase of the motor to investigate the performance.

It is possible to calculate the motor force using Finite Element Methods. However, before using those complex programs, we want to use a simple magnetic circuit model, like Ostovic et al [2]. Magnetomotive forces represent the currents and the magnets. The saturating parts of the magnetic circuit are modelled as variable reluctances.

Figure 1 depicts a schematic section of the linear permanent-magnet motor. Table 1 lists some important dimensions. Figure 2 depicts a photo. The magnets are on the bottom plate. The translator has a fractional pitch winding with the following advantages.

- The winding consists of coils around a tooth with simple and short end windings that can be wound outside the motor.
- The orthocyclic method of coil winding described by Lenders [3] can be used, which results in a high copper filling factor of the slots.
- The translator yoke and the back-iron behind the magnets can be thin.

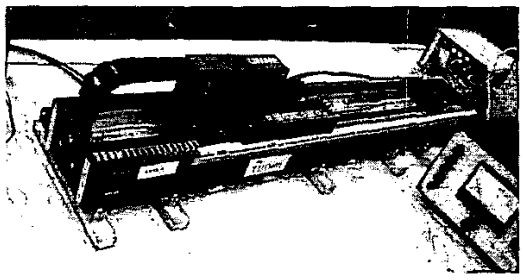

Figure 2: Photo of the linear permanent-magnet motor with bottom plate with magnets and translator with coils.

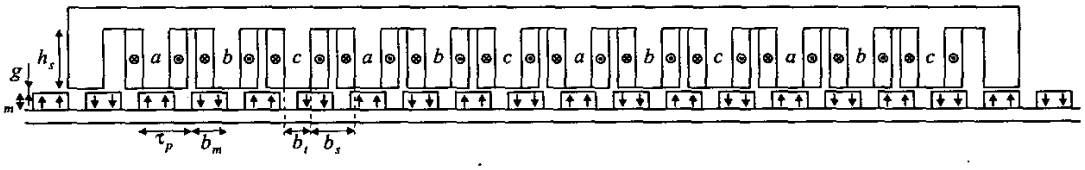

Figure 1: Section of the linear permanent-magnet motor with some dimensions.

Power Electronics, Machines and Drives, 16-18 April 2002,
Conference Publication No.487, © IEE 2002

In figure 1, a phase consist of four series-connected coils. When the translator moves over the magnets, a three-phase voltage is induced in the coils. This voltage is almost sinusoidal due to the skewing of the magnets and due to the end teeth. A position sensor detects the position of the translator. Based on this position information, a power amplifier generates a three-phase sinusoidal current.

TABLE 1: Some dimensions from figure 1.

description	symbol	size
pole pitch	τ_p	12 mm
magnet thickness	h_m	4 mm
magnet width	b_m	8 mm
magnet length	l_m	60 mm

2 MAGNETIC CIRCUIT MODELLING

Equivalent magnetic circuit model

In this section, a magnetic circuit model of the linear motor is derived. In this model, the magnetic fluxes in the teeth are the most important, because these fluxes link with the stator coils which are used in the force calculation.
In order to obtain a simple model, end effects and end teeth are neglected, so that it is sufficient to consider three translator teeth. It is further assumed that only the translator teeth (around which the coils are wound) saturate. Because the translator yoke and the back-iron of the bottom plate are thick, the reluctance of the translator yoke and the back-iron is negligible. The resulting model is given in figure 3.

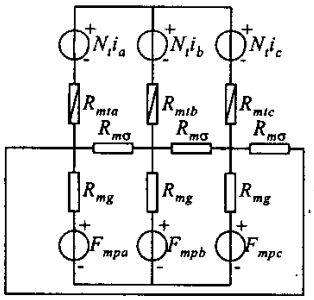

Figure 3: Simplified magnetic circuit model of the linear PM motor.

Reluctance values

A general expression for the value of a reluctance is

$$R_m = \frac{l_c}{A_c}\frac{H}{B} \qquad (1)$$

where
H is the magnetic field intensity in the circuit,
B is the magnetic flux density in the circuit,
l_c is the length of the magnetic circuit, and
A_c is the cross-section of the magnetic circuit.
With this, the air gap reluctance R_{mg} (the reluctance between a tooth and the back iron) can be expressed as

$$R_{mg} = \frac{g + h_m/\mu_{rm}}{2\mu_0 b_t l_s} \qquad (2)$$

where
g is the air gap length,
μ_{rm} is the recoil permeability of the magnets,
μ_0 is the magnetic permeability in vacuum,
b_t is the tooth width, and
l_s is the stack length, the length in the direction perpendicular to the plane of the drawing in figure 1.
The width of the flux path is chosen twice the tooth width because the flux crosses the air gap not only below the tooth, but in a much wider path due to flux fringing.
The slot leakage reluctance $R_{m\sigma}$ is calculated as

$$R_{m\sigma} = \frac{2b_s}{\mu_0 h_s l_s} \qquad (3)$$

where
b_s is the slot width, and
h_s is the slot height.
Half the slot height is used in the circuit surface because the leakage flux density in the slot increases from zero close to the yoke to a maximum close to the air gap.
The starting point for the determination of the tooth reluctance is the *BH*-curve of the magnetic material measured by Jansen [4] and depicted in figure 4. This *BH*-curve is approximated with a function which is also depicted in figure 4:

$$H = 150B + 15B^{11} \qquad (4)$$

If we use this expression in the general expression for a reluctance, we obtain the tooth reluctance R_{mt} as

$$R_{mt} = \frac{2h_s}{3b_t l_s}(150 + 15B_t^{10}) \qquad (5)$$

In this equation, the circuit surface is the cross-section of a tooth, and the length is taken as two third of the tooth height. Two third of the tooth height is taken because leakage flux enters the tooth over the whole height, so that the lower part does not saturate.

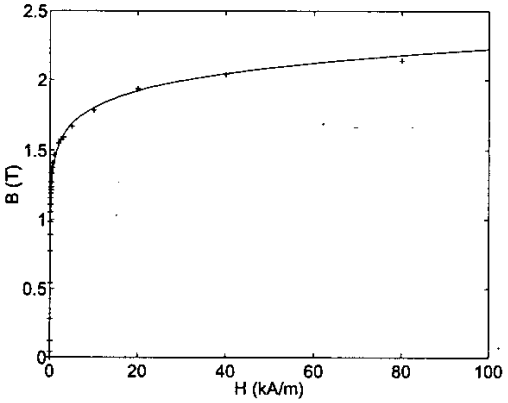

Figure 4: Measured BH-curve of the magnetic material (+) and the approximation used in the calculations.

Magnetomotive forces

The magnetomotive force of a translator current equals the phase current multiplied by the number of turns of the coil around a translator tooth N_t.

The magnets also cause a flux in the translator teeth. To calculate the magnetomotive force of the magnets, we start with calculating the flux in the translator teeth in the linear, non-saturated case. When the translator is in the position of figure 2, the flux in tooth *a* due to the magnets is maximum. Because the flux paths close via teeth *b* and *c* and because of the symmetry, the flux in teeth *b* and *c* is minus half the flux in tooth *a*.

We assume the flux to cross the air gap and the magnets perpendicular at the places where a tooth overlaps a magnet and to be zero where this is not the case. With this assumption, the flux density in the gap between an overlapping magnet and tooth is equal in all gaps because the overlap area below tooth *a* is equal to the overlap area of tooth *b* and *c* together. Therefore, the flux density can be calculated from Ampère's law:

$$\oint \vec{H}\cdot d\vec{l} = \int\int \vec{J}\cdot d\vec{A} \quad \rightarrow \quad H_m h_m + H_g g = 0 \tag{6}$$

where

H_m is the magnetic field strength in the magnet, and

H_g is the magnetic field strength in the air gap.

In this equation we substitute the relations between the magnetic flux density B and the magnetic field strength H in the air gap and in the magnet:

$$B_g = \mu_0 H_g \tag{7}$$

$$B_m = \mu_0 \mu_{rm} H_m + B_{rm} \tag{8}$$

where B_{rm} is the remanent flux density of the magnets. Further, we use the magnetic flux continuity:

$$B_g = B_m \tag{9}$$

With this, the air gap flux density can be calculated as

$$B_g = B_{rm}\frac{h_m}{h_m + \mu_{rm} g} \tag{10}$$

The flux entering the tooth is this flux density multiplied by the area of the tooth. Some extra flux will enter the tooth, because the magnets are wider than the tooth. On the other hand, the magnets are skewed, which results in a reduction of the maximum flux. Here, the maximum flux $\hat{\Phi}_{pm}$ is calculated as

$$\hat{\Phi}_{pm} = B_{rm}\frac{h_m}{h_m + \mu_{rm} g} b_t l_s \tag{11}$$

The flux varies sinusoidally, as can be concluded from the sinusoidal form of the no-load voltages. Hence, the fluxes in the translator teeth due to the magnets are given by

$$\begin{aligned}
\Phi_{pma} &= \hat{\Phi}_{pm}\cos\left(\frac{\pi}{\tau_p}x\right) \\
\Phi_{pmb} &= \hat{\Phi}_{pm}\cos\left(\frac{\pi}{\tau_p}x - \frac{2}{3}\pi\right) \\
\Phi_{pmc} &= \hat{\Phi}_{pm}\cos\left(\frac{\pi}{\tau_p}x - \frac{4}{3}\pi\right)
\end{aligned} \tag{12}$$

where x is the translator position, which is zero in figure 1.

This rather rough estimate of the flux leads to good results, as appears from the measurements reported later in section 4, table 2.

In principle, this flux follows a path different from the path followed by the flux caused by the translator currents and the reluctance is different from the air gap reluctance. However, for our model, only the flux entering the stator teeth is of interest. Therefore, the magnetomotive force of the magnets is modelled as

$$\begin{aligned}
F_{mpma} &= R_{mg}\Phi_{pma} \\
F_{mpmb} &= R_{mg}\Phi_{pmb} \\
F_{mpmc} &= R_{mg}\Phi_{pmc}
\end{aligned} \tag{13}$$

When the teeth saturate, the fluxes caused by the magnets decrease, but the magnetomotive forces remain equal.

Voltage equations

The voltages of the translator phases can be written as

$$\begin{aligned}
u_a &= Ri_a + \frac{d\lambda_a}{dt} = Ri_a + N_s\frac{d\Phi_a}{dt} \\
u_b &= Ri_b + \frac{d\lambda_b}{dt} = Ri_b + N_s\frac{d\Phi_b}{dt} \\
u_c &= Ri_c + \frac{d\lambda_c}{dt} = Ri_c + N_s\frac{d\Phi_c}{dt}
\end{aligned} \tag{14}$$

where

R is the phase resistance,

i_a is the phase current of phase *a*,

λ_a is the flux linkage of phase *a*,

Φ_a is the flux in a tooth of phase *a*, and

N_s is the total number of turns of a phase.

Because some elements in the magnetic circuit are non-linear due to saturation, the equations for the fluxes have to be solved by means of an iteration process.

In the rest of this subsection, the voltage equations are worked out for the case that the currents are so low that the magnetic circuit does not saturate. In this case, the flux linkage can be seen as a superposition of the flux linkage due to the magnets and the flux linkage due to the translator currents:

$$\begin{aligned}
\lambda_a &= Li_a + Mi_b + Mi_c + N_s\Phi_{pma} \\
\lambda_b &= Mi_a + Li_b + Mi_c + N_s\Phi_{pmb} \\
\lambda_c &= Mi_a + Mi_b + Li_c + N_s\Phi_{pmc}
\end{aligned} \tag{15}$$

where

L is the self-inductance of a phase, and

M is the mutual inductance between two phases.

From the magnetic circuit, it can be concluded that

$$L = \frac{N_s}{N_t}\frac{\frac{N_t^2}{1}}{\frac{2}{3R_{mg}} + \frac{2}{R_{m\sigma}}} = N_s N_t \frac{2R_{m\sigma} + 6R_{mg}}{3R_{mg}R_{m\sigma}} \tag{16}$$

where N_t is the number of turns of a coil around a tooth. The term N_s/N_t in the first expression is there to take the other teeth of the same phase into account.

In the same way, it can be concluded that

$$M=-\frac{1}{2}L \tag{17}$$

If we also take into account that there is no star-point connection (so that the sum of the currents is zero), the voltage equations can be written as

$$\begin{aligned}
u_a &= Ri_a+\frac{3}{2}L\frac{di_a}{dt}-N_s\frac{\pi}{\tau_p}\hat{\Phi}_{pm}\sin(\frac{\pi}{\tau_p}x)\frac{dx}{dt}\\
u_b &= Ri_b+\frac{3}{2}L\frac{di_b}{dt}-N_s\frac{\pi}{\tau_p}\hat{\Phi}_{pm}\sin(\frac{\pi}{\tau_p}x-\frac{2}{3}\pi)\frac{dx}{dt}\\
u_c &= Ri_c+\frac{3}{2}L\frac{di_c}{dt}-N_s\frac{\pi}{\tau_p}\hat{\Phi}_{pm}\sin(\frac{\pi}{\tau_p}x-\frac{4}{3}\pi)\frac{dx}{dt}
\end{aligned} \tag{18}$$

Again it is mentioned that in these equations, saturation is neglected.

3 FORCE CALCULATIONS

Power balance

A thorough description of the derivation of the force from a power balance is given by Fitzgerald et al [5].
The starting point for this force calculation is the power balance:

$$p_e=p_m+\frac{dW_m}{dt}+p_d \tag{19}$$

where
W_m is the magnetic energy stored in the system,
p_e is the electric power going into the system:

$$p_e=i_a u_a+i_b u_b+i_c u_c \tag{20}$$

p_d is the electric dissipation in the system:

$$p_d=Ri_a^2+Ri_b^2+Ri_c^2 \tag{21}$$

p_m is the mechanical power generated by the system:

$$p_m=F_{em}\frac{dx}{dt} \tag{22}$$

where F_{em} is the electro mechanic force generated by the motor.
In this power balance, iron losses are neglected.

Force in the linear model

If the currents are so low that the teeth do not saturate, (18) can be substituted in (20). If then (20), (21), and (22) are substituted in (19), and it is noticed that

$$\frac{dW_m}{dt}=i_a\frac{3}{2}L\frac{di_a}{dt}+i_b\frac{3}{2}L\frac{di_b}{dt}+i_c\frac{3}{2}L\frac{di_c}{dt} \tag{23}$$

the resulting force is calculated as

$$\begin{aligned}
F_{em}=-N_s\frac{\pi}{\tau_p}\hat{\Phi}_{pm}(i_a\sin(\frac{\pi}{\tau_p}x)+i_b\sin(\frac{\pi}{\tau_p}x-\frac{2}{3}\pi)\\
+i_c\sin(\frac{\pi}{\tau_p}x-\frac{4}{3}\pi))
\end{aligned} \tag{24}$$

When the three phase currents are given by

$$\begin{aligned}
i_a &= -\hat{i}\sin(\frac{\pi}{\tau_p}x+\varphi)\\
i_b &= -\hat{i}\sin(\frac{\pi}{\tau_p}x-\frac{2}{3}\pi+\varphi)\\
i_c &= -\hat{i}\sin(\frac{\pi}{\tau_p}x-\frac{4}{3}\pi+\varphi)
\end{aligned} \tag{25}$$

the force is calculated as

$$F_{em}=\frac{3}{2}\frac{\pi}{\tau_p}N_s\hat{\Phi}_{pm}\hat{i}\cos\varphi \tag{26}$$

Force under saturated conditions

If the currents are higher and the magnetic circuit saturates, the general voltage equation (14) must be used. If this equation is substituted in (20), and subsequently (20), (21), and (22) are substituted in (19), we obtain

$$i_a\frac{d\lambda_a}{dt}+i_b\frac{d\lambda_b}{dt}+i_c\frac{d\lambda_c}{dt}=\frac{dW_m}{dt}+F_{em}\frac{dx}{dt} \tag{27}$$

In the non-linear saturating case, it is useful to introduce the coenergy W_m' for the calculation of the force as in [5]. The coenergy is introduced here as

$$W_m'=i_a\lambda_a+i_b\lambda_b+i_c\lambda_c-W_m \tag{28}$$

When this equation is rewritten as

$$W_m=i_a\lambda_a+i_b\lambda_b+i_c\lambda_c-W_m' \tag{29}$$

and substituted in equation (27), the result can be worked out to

$$\frac{dW_m'}{dt}=\lambda_a\frac{di_a}{dt}+\lambda_b\frac{di_b}{dt}+\lambda_c\frac{di_c}{dt}+F_{em}\frac{dx}{dt} \tag{30}$$

If the coenergy is assumed to be a function of the three phase currents and the position, it can be written as

$$\frac{dW_m'}{dt}=\frac{\partial W_m'}{\partial i_a}\frac{di_a}{dt}+\frac{\partial W_m'}{\partial i_b}\frac{di_b}{dt}+\frac{\partial W_m'}{\partial i_c}\frac{di_c}{dt}+\frac{\partial W_m'}{\partial x}\frac{dx}{dt} \tag{31}$$

From comparing (30) and (31), it can be concluded that

$$F_{em}=\frac{\partial W_m'}{\partial x} \tag{32}$$

This equation gives a well-known relation between the coenergy and the electromagnetic force [5].
To calculate the force from this equation, the coenergy has to be determined, which can be done by integrating equation (30). The contribution of last term of equation (30) to the integration is zero when the position does not change or when the force is zero when the currents are zero. The integration then results in:

$$\begin{aligned}
W_m'(i_a,i_b,i_c,x)=\int_0^{i_a}\lambda_a(i_a',0,0,x)di_a'+\int_0^{i_b}\lambda_b(i_a,i_b',0,x)di_b'\\
+\int_0^{i_c}\lambda_c(i_a,i_b,i_c',x)di_c'+W_{m0}'(x)
\end{aligned} \tag{33}$$

where $W_{m0}'(x)$ is the magnetic coenergy when the currents are zero.

Because it is difficult to solve the equations (32) and (33) analytically, they are determined numerically. Therefore, equation (32) is rewritten to

$$F_{em}=\frac{W'_m(x+\Delta x)-W'_m(x)}{\Delta x} \qquad (34)$$

It is assumed that $W'_{m0}(x)$ is not a function of x. That this assumption is reasonable, appears from the fact that when the translator is moved over the magnets, the cogging force is very small (below 1% of the peak force). With this assumption, the problem that $W'_{m0}(x)$ in (33) is not known is solved, because it is present at both sides of the minus sign of equation (34).

4 THEORETIC AND EXPERIMENTAL RESULTS

Parameters

Table 2 compares some calculated and measured quantities. The measurements have been done with zero or small currents, so that the magnetic circuit is not saturated. The measured maximum value of the no-load flux linkage $\hat{\lambda}_{pm}$ is obtained from integrating the measured no-load voltage over time.

The inductance $3/2L$ is overestimated. This is probably caused by the fact that in the model, the complete leakage flux links with all the turns of the coil, while in reality, the turns are distributed over the tooth height, so that a part of the leakage flux does not link with all turns.

TABLE 2: Comparison of calculated and measured quantities under non-saturated conditions.

	Calculated	Measured
$\hat{\lambda}_{pm}=N_s\hat{\Phi}_{pm}$ (mWb)	188	185
$3/2L$ (mH)	33	28
$F_{em}/\hat{i}$ (N/A)	74	73

Force as a function of current amplitude

Figure 5 depicts the calculated force as a function of current amplitude and position. The three phase currents are made a function of the position as in (25) with $\varphi=0$ to maximize the force.

The calculations show that the force becomes a function of the position when the motor saturates. This function is periodic every 4 mm (one third of a pole pitch). This is reasonable, because when the translator moves, three times per pole pitch magnetically the same situation occurs.

Figures 6 and 7 depict the calculated respectively the measured ratio of force divided by current amplitude as a function of the current amplitude and the position. In figure 8, measured and calculated values are depicted.

The ratio of force to current amplitude stays more or less constant for current amplitudes up to about 7 A, but when the current increases further to 16 A, this ratio decreases substantially due to saturation.

The correlation between measurements and calculations is reasonable. The decrease of the force is in the same order of magnitude as calculated. Also the measured force becomes a periodic function of the position.

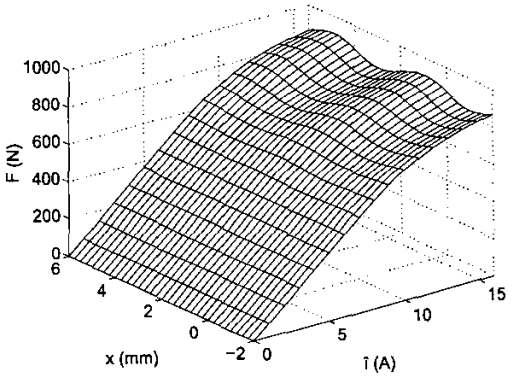

Figure 5: Calculated force as a function of current amplitude and position.

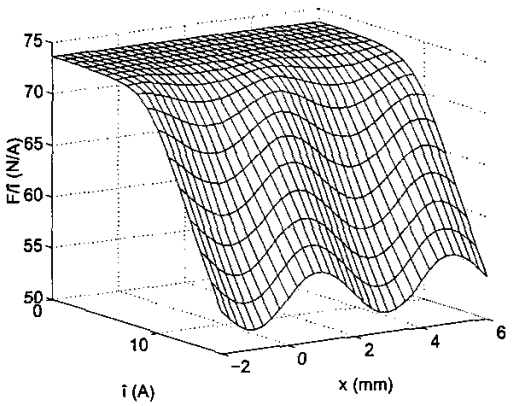

Figure 6: Calculated ratio of force divided by current amplitude as a function of current amplitude and position.

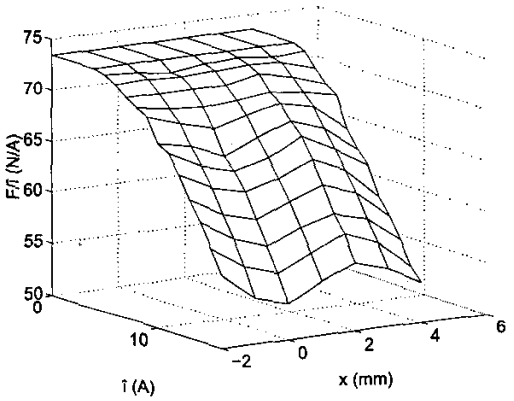

Figure 7: Measured ratio of force divided by current amplitude as a function of current amplitude and position.

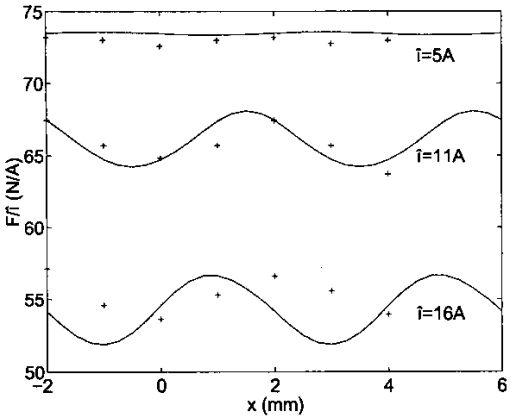

Figure 8: Measured (+) and calculated (-) ratio of force divided by current amplitude as a function of the position for three different current amplitudes.

However, as appears from figure 8, the measured force variation as a function of the position seems to be smaller than the calculated. Also the position of the minimum and the maximum seems to be different. This might be caused by measuring inaccuracies, by end effects, or by inaccurate estimates in the model.

Force as a function of phase angle

Figure 9 depicts the force as a function of the position and the phase angle φ at a current amplitude of 16 A. From this figure, a few interesting conclusions can be drawn:

- The amplitude of the variation as a function of the position decreases when the phase angle φ increases.
- The force generated with this current amplitude at φ=15° is about 3% higher than at φ=0.

This can be explained from the fact that a leading current reduces the flux levels in the teeth, thus reducing the saturation level.

This observation could make it attractive to have a current leading the no-load voltage when the motor is saturated.

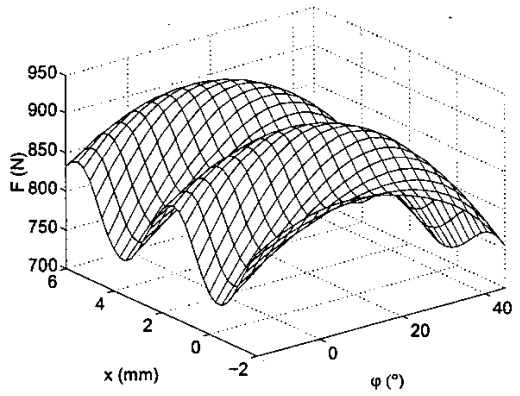

Figure 9: Calculated force as a function of position and phase angle φ at a current amplitude of 16 A.

Force density

The peak force that can be generated with this motor is over 800 N. If the force density is defined as the force divided by the active air-gap area (stack length multiplied by 12 times the slot pitch), the air gap force density is about 8 N/cm^2. This is quite high. This peak force is mainly limited by the demagnetization properties of the magnets and by saturation.

If the motor has an aluminium heat sink (as in figure 2) and is cooled by natural convection, the continuous force is about 340 N, which means a force density of about 3.4 N/cm^2.

There are some possibilities to increase the force further.

- If cobalt iron is used in the magnetic circuit instead of silicon iron, the saturation flux density may increase with 30 %.
- Stronger magnets can be used.
- Halbach array magnets can be used.

With a combination of these measures, an increase of both the peak and the continuous force with 30% should be possible.

5 CONCLUSIONS

This paper shows that it is possible to model a linear permanent-magnet motor including saturation using magnetic circuit theory. The results can be used to improve the feed-forward position control of the system. The applied linear PM motor with fractional slot winding can achieve high continuous and peak force densities. In saturation, a current leading the no-load voltage reduces the flux level in the motor, which results in an increase of the generated force. The reasonable correlation between the calculated and the measured parameters and forces justifies the model.

ACKNOWLEDGEMENT

The authors want to thank Mr A.T.A. Peijnenburg, Philips CFT, Eindhoven, for providing them with the linear PM motor for the experimental work.

REFERENCES

[1] J.F. Gieras, Z.J. Piech, "Linear synchronous motors: transportation and automation systems", Boca Raton: CRC Press, 2000.

[2] V. Ostovic, J.M. Miller, V.K. Grag, R.D. Schultz, S.H. Swales, "A magnetic-equivalent-circuit-based performance computation of a Lundell alternator", in IEEE Transactions on Industry Applications, 1999 (vol. 35), No 4, pp. 825-830.

[3] W. Lenders, "The orthocyclic method of coil winding", in Philips Technical Review, 1961/1962 (Vol. 23), No. 12, pp. 365-404.

[4] J. Janssen, "Materials Library", Third edition, Philips Report CTR505-90-RJ261, 1990.

[5] A.E. Fitzgerald, C. Kingsley, S.D. Umans, "Electric machinery", Fifth edition, London: McGraw-Hill, 1990.